EVALUATION OF THE SEISMIC PERFORMANCE IN CONFINED MASONRY DWELLINGS RETROFITTED WITH STEEL MESH AND CEMENT-SAND MORTAR

EVALUACIÓN DEL DESEMPEÑO SÍSMICO DE VIVIENDAS DE ALBAÑILERÍA CON REFORZAMIENTO DE MALLA DE ACERO Y MORTERO CEMENTO-ARENA

Luis Lopez[1,2]*, Miguel Diaz[1,2], Erika Flores[1,2], Michel Amancio[1,2], Steven Roman[1,2]

[1] *Japan-Peru Center for Earthquake Engineering Research and Disaster Mitigation, Lima, Peru*

[2] *Faculty of Civil Engineering, National University of Engineering, Lima, Peru*

Received (Recibido): 12 / 03 /2025 Publicado (Published): 30 / 12 / 2025

ABSTRACT

Field studies conducted by the Japan–Peru Center for Earthquake Engineering Research and Disaster Mitigation (CISMID) in 2019 indicate that 83% of dwellings in Metropolitan Lima are constructed with masonry. Lima is a highly earthquake-prone area due to its location along the Pacific Ring of Fire, where recurrent seismic events pose a significant threat to residential buildings. A large portion of these dwellings are non-engineered, built without professional supervision or proper material quality control, which increases their seismic vulnerability. This study aims to evaluate the effectiveness of a retrofitting technique based on the application of a steel mesh and a cement–sand mortar overlay in confined masonry dwellings in Metropolitan Lima. Fourteen non-engineered dwelling typologies were analyzed, considering five wall densities and two structural conditions, retrofitted and non-retrofitted. Scaled seismic records for six demand levels on rigid (S1) and intermediate (S2) soils were used following the criteria of ASCE 41-13 and the Peruvian Seismic Code (E.030). Capacity curves were developed, showing increases in shear strength and lateral deformation capacity for the retrofitted typologies. Damage indices were defined to normalize drift into a 0–5 scale. A total of 5,880 nonlinear time-history analyses were performed. The results show that non-retrofitted dwellings lack sufficient capacity to withstand the rare seismic event, defined by a 5% probability of exceedance in 50 years and a 975-year return period, expected in Lima due to its prolonged seismic silence. Under this level of intensity, only 10% of non-retrofitted dwellings maintain adequate seismic performance, while retrofitting increases this proportion to 73%, demonstrating a substantial improvement in seismic capacity.

Keywords: Seismic Demand, Dwelling Typologies, Simulations, Retrofitting, Damage Indices.

RESUMEN

Los estudios de campo realizados por el Centro Peruano–Japonés de Investigaciones Sísmicas y Mitigación de Desastres (CISMID) en 2019 indican que el 83% de las viviendas en Lima Metropolitana están construidas con albañilería. Lima es una zona altamente propensa a sismos por su ubicación en el Cinturón de Fuego del Pacífico, donde los eventos recurrentes representan una amenaza significativa para las edificaciones. Una parte importante corresponde a viviendas no ingenieriles, construidas sin supervisión profesional ni adecuado control de calidad de materiales, lo que incrementa su vulnerabilidad sísmica. Este estudio tiene como objetivo evaluar la efectividad de un refuerzo basado en la aplicación de una malla de acero y un recubrimiento de mortero cemento–arena en viviendas de albañilería confinada de Lima Metropolitana. Se analizaron catorce tipologías de viviendas no ingenieriles, considerando cinco densidades de muro y dos condiciones estructurales, reforzadas y no reforzadas. Se emplearon registros sísmicos escalados para seis niveles de demanda sobre suelos rígidos e intermedios, siguiendo los criterios de ASCE 41-13 y la Norma Sísmica Peruana E.030. Se calcularon curvas de capacidad, mostrando incrementos en la resistencia cortante y capacidad de deformación lateral en viviendas reforzadas. Se definieron índices de daño para normalizar la distorsión en una escala de 0 a 5. En total, se realizaron 5,880 simulaciones tiempo-historia no lineales. Los resultados muestran que las viviendas no reforzadas no poseen capacidad suficiente para resistir el sismo raro, caracterizado por una probabilidad de excedencia del 5% en 50 años y un periodo de retorno de 975 años, esperado en Lima debido a su prolongado silencio sísmico. Bajo esta intensidad, solo el 10% de las viviendas sin reforzamiento mantiene un comportamiento sísmico adecuado, mientras que el reforzamiento eleva esta proporción al 73%, evidenciando una mejora significativa en la capacidad sísmica.

Palabras Clave: Demanda Sísmica, Tipologías de Viviendas, Simulaciones Sísmicas, Reforzamiento, Niveles de Daño.

[1] * Corresponding author:
E-mail: lflopezr@uni.pe

1. INTRODUCTION

Non-engineered confined masonry dwellings are the predominant residential structural system in Metropolitan Lima and Callao, as reported by recent field surveys conducted by CISMID [1]. These dwellings commonly exhibit marked structural irregularities, particularly due to the use of different brick types across stories: handmade solid bricks on the first floor and industrial hollow (tubular) bricks on upper floors. Both materials fail to satisfy the lateral drift limits prescribed by the Peruvian Seismic Code E.030, with tubular bricks presenting significantly lower deformation and axial capacities [2]. As a consequence, these dwellings develop different interstory drift limits along their height, and the story containing tubular bricks typically governs the onset of collapse. Given the high seismic hazard in Lima, this configuration results in substantial seismic vulnerability.

Previous experimental and analytical studies have documented these deficiencies. Zavala [3] demonstrated that handmade solid-brick dwellings may achieve drift ratios beyond those specified in Standard E.070, yet still present critical deformation limitations. Salinas and Lazares [4] showed that hollow-brick dwellings do not meet the drift requirements of Standard E.030, confirming their high susceptibility to damage. Díaz [5] introduced a retrofitting technique using steel mesh and a cement–sand mortar overlay, demonstrating significant improvements in wall strength, stiffness, and ductility, and showing that retrofitted dwellings remain within acceptable drift limits even under severe seismic demands. Additionally, Zavala [6] proposed new drift ratio limits for different brick types and identified drift thresholds associated with distinct limit states in confined masonry walls. Collectively, these studies underscore the urgent need for reliable, scalable retrofitting solutions for non-engineered masonry dwellings in Peru.

While previous studies have investigated the behavior of confined masonry dwellings with and without retrofitting, the present research extends the range of wall-density cases considered for both structural conditions and provides a detailed methodological framework that enables full reproducibility of the analysis. By incorporating a broader set of dwelling configurations and documenting each step of the seismic performance assessment, this study offers an expanded and systematic evaluation of typologies commonly found in Metropolitan Lima.

The objective of this study is to evaluate the effectiveness of a steel mesh and cement–sand mortar overlay applied to confined masonry dwelling typologies. The analysis includes the development of capacity curves, the computation of drift-based damage indices, and nonlinear time-history simulations under six seismic demand levels for S1 and S2 soil conditions. The outcomes contribute to improving seismic risk mitigation strategies for low-income, non-engineered housing in highly seismic regions [7], [2].

2. METHODOLOGY

Fig. 1 presents a summary of the methodological workflow adopted in this study. The flowchart organizes the analysis into its principal stages: definition of input data, processing and scaling of seismic records, characterization of dwelling typologies, development of capacity curves for both unretrofitted and retrofitted dwellings, and the execution of nonlinear time-history analyses.

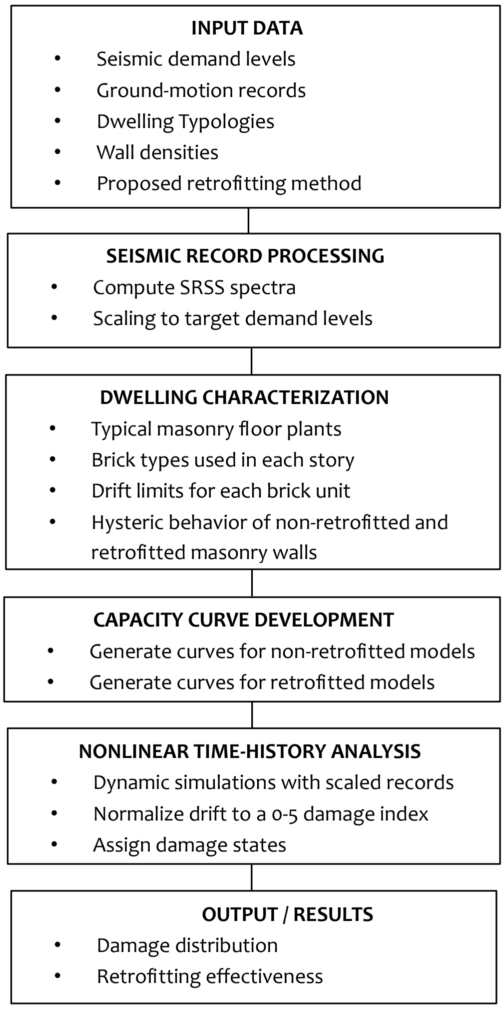

Fig. 1. Workflow of the Seismic Performance Assessment.

2.1. SEISMIC DEMAND IN METROPOLITAN LIMA AREA

The study area is located in Seismic Zone 4 according to the Peruvian Standard E.030 [8]. The seismic demand categories used in this study *Very Slight, Slight, Moderate, Severe, Rare,* and *Very Rare* follow the classification introduced in previous CISMID research [5], [9]. These qualitative categories correspond to the probabilistic ground-motion levels defined in ASCE 41-23 [10], as summarized in Table I. The corresponding peak ground accelerations (Z values) are taken from the seismic hazard studies conducted by CISMID for Metropolitan Lima [11].

The selection of ground-motion records was based on criteria representative of the seismic environment of Metropolitan Lima. The dataset includes interplate and intraplate events with magnitudes between 6.6 and 8.1, consistent with the subduction earthquakes that govern the seismic hazard of central Peru. The records were obtained from stations located on rigid (S1) and intermediate (S2) soils, ensuring compatibility with the soil conditions of the study area. Each record was validated according to its signal quality, recording completeness, and the clear identification of source mechanism and depth. Additionally, the selected events exhibit spectral characteristics compatible with the Peruvian design spectra, and their peak ground accelerations fall within the range of significant values observed in regional strong-motion events. A synthetic record was included to complement the dataset for S1 soil conditions. All accelerograms were retrieved from the REDACIS and CISMID strong-motion databases [12].

The simulations incorporated six real seismic records and one synthetic record, where four records correspond to rigid soil (S1) and three to intermediate soil (S2), as is detailed in Table II. Each seismic record was scaled according to the Peruvian Standard E.030 to match the specified seismic demand levels.

TABLE I
Maximum accelerations in rigid soil in the study area with probability of exceedance according to [5], [9].

Seismic Demand	Probability of Exceedance	Return Period (years)	Z* (g)
Very slight	50%/30 years	43	0.15
Slight	50%/50 years	72	0.20
moderate	20%/50 years	225	0.33
Severe	10%/50 years	475	0.45
Rare	5%/50 years	975	0.58
Very Rare	2%/50 years	2475	0.78

Note: *According to CISMID's seismic hazard studies [11].

The components of each seismic record exhibiting the highest peak ground acceleration were selected for the simulations. These components were normalized to a unit PGA prior to scaling and are shown in Fig. 2–Fig. 8.

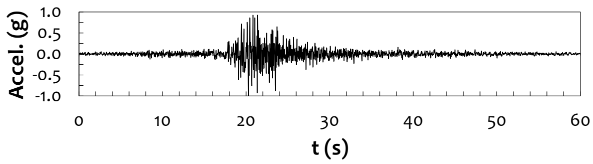

Fig. 2. Normalized seismic record, Lima_17/Oct/1966, NS component.

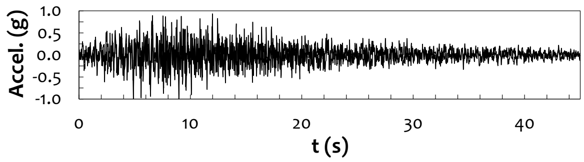

Fig. 3. Normalized seismic record, Huaraz_31/May/1970, EW component.

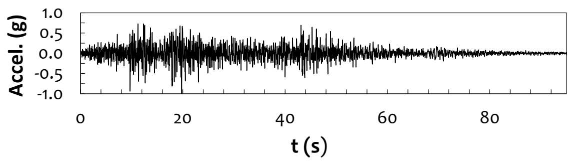

Fig. 4. Normalized seismic record, Lima_03/Oct/1974, EW component.

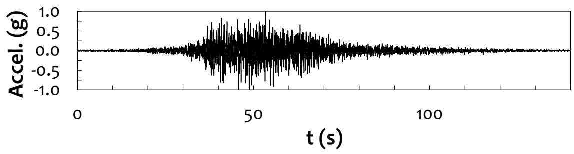

Fig. 5. Normalized seismic record, Arequipa_23/Jun/2001, EW component.

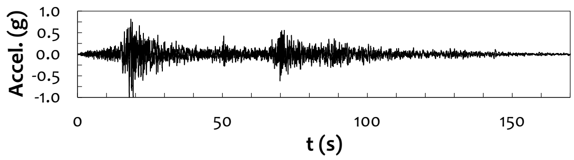

Fig. 6. Normalized seismic record, Pisco_15/Aug/2001, NS component.

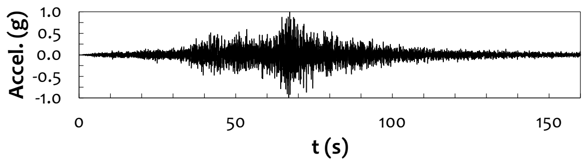

Fig. 7. Normalized seismic record, Lagunas_26/May/2019, EW component.

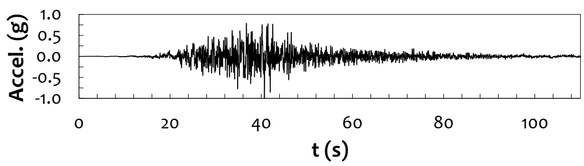

Fig. 8. Normalized synthetic seismic record, SATREPS, EW component.

TABLE II
Characteristics of seismic records employed in seismic simulations.

Record	Station	Soil Profile Type	PGA EW (cm/s²)	PGA NS (cm/s²)	Magnitude	Deep (Km)
Lima_17/Oct/1966	Parque de la Reserva	S1	175	268	8.1 Mw	24
Huaraz_31/May/1970	Parque de la Reserva	S1	105	98	6.6 Mb	64
Lima_03/Oct/1974	Parque de la Reserva	S1	190	169	6.6 Mb	13
Arequipa_23/Jun/2001	César Vizcarra	S2	289	229	8.4 Mw	33
Pisco_15/Ago/2007	UNICA	S2	293	367	7.9 Mw	40
Lagunas_26/May/2019	SCIQU	S2	82	74	7.2 ML	141
Sintético, SATREPS	-	S1	606	-	-	-

Note: Source REDACIS - CISMID.

Fig. 9 presents the Square Root of the Sum of Squares (SRSS) spectra with a 5% damping ratio for the seismic records listed in Table II, grouped according to soil type. The results indicate that spectral amplification occurs before the soil period Tp, followed by a reduction in spectral ordinates thereafter. The SRSS spectra were used to scale the seismic records employed in the simulations for each seismic demand level defined in Table I.

All dwelling typologies listed in Table IV, along with their corresponding wall densities, were analyzed using the same set of ground-motion records described in Table II. This uniform selection ensures methodological consistency and allows isolating the influence of structural parameters—such as brick type, wall density, and retrofit condition—without introducing variability from different input motions. The use of a common suite of real and synthetic accelerograms is appropriate because all typologies represent low-rise confined masonry dwellings located within the same seismic environment of the Metropolitan Lima area. The scaling of the records was performed using the Z·S reference acceleration of the Peruvian Standard E.030, which prevents unrealistically large spectral amplifications that arise when enforcing full-spectrum compatibility. The confined masonry dwellings analyzed in this study have fundamental periods ranging approximately from 0.10 s for one-story buildings to 0.50 s for five-story buildings. Therefore, a representative period of 0.30 s was selected for scaling, as it lies near the midpoint of this range and adequately captures the dynamic behavior of the dwelling typologies considered. Scaling the records to match the target spectral outside this governing range have negligible influence on low-rise masonry response. Consequently, the observed differences in seismic performance are attributed to the structural characteristics of each typology rather than to inconsistencies in the ground-motion input.

The seismic parameters were obtained from the Peruvian Standard E.030 and were used to generate

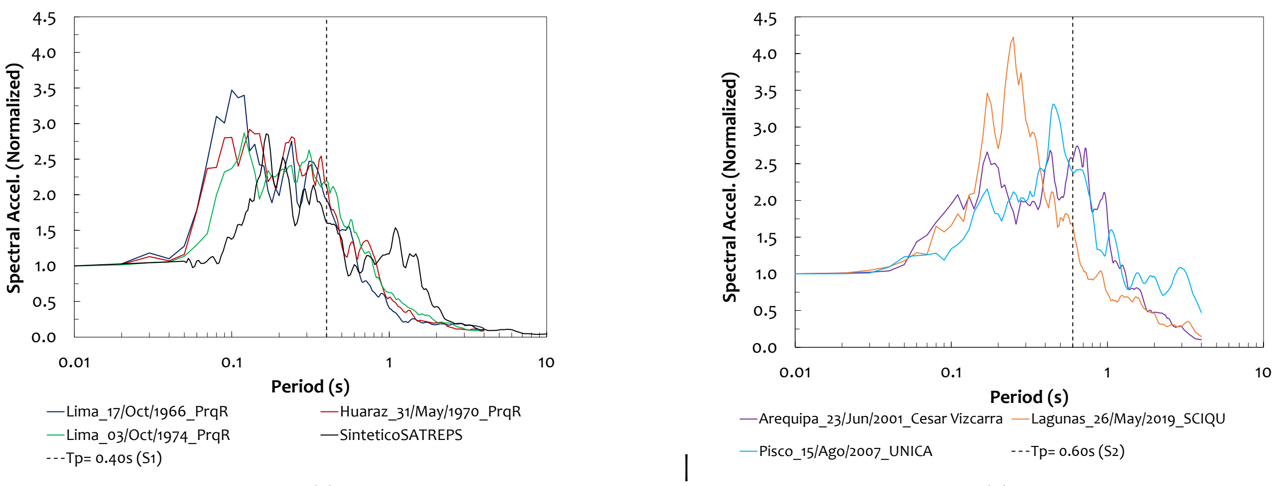

(a) (b)

Fig. 9. Normalized SRSS spectra of seismic records. (a) On rigid soil (S1). (b) On intermediate soil (S2).

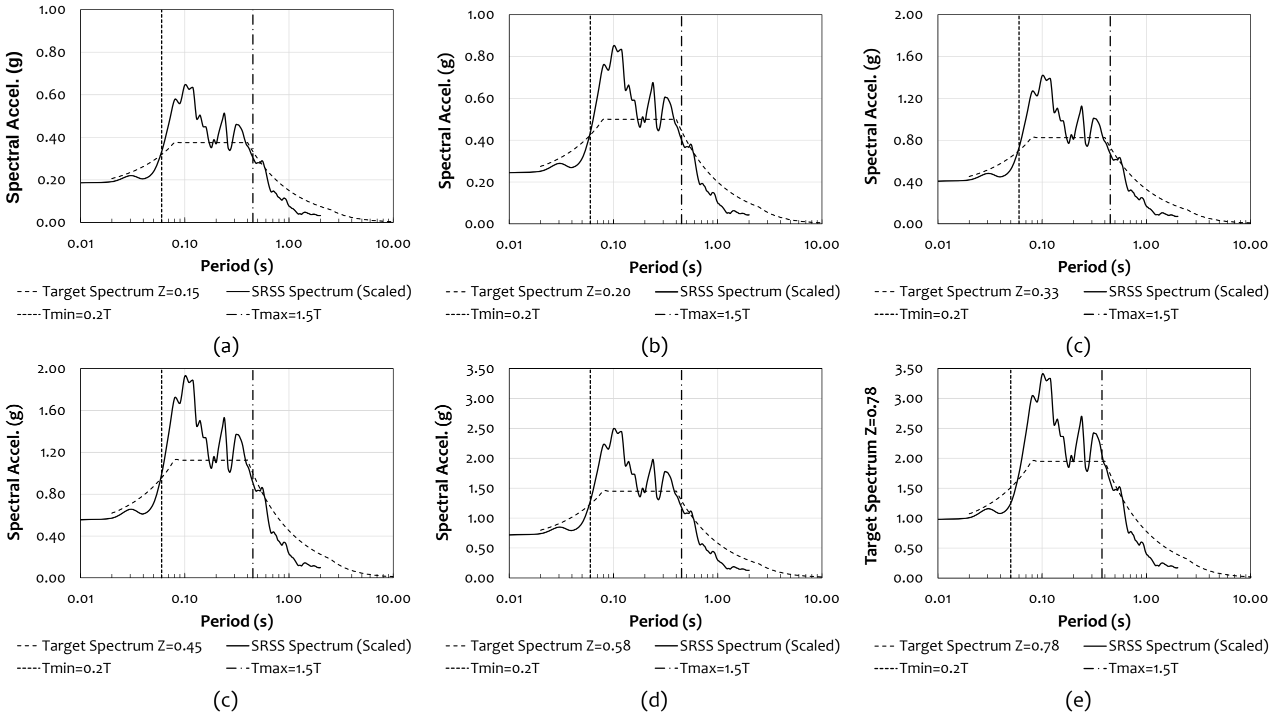

Fig. 10. Scaling of seismic records for the seismic demands in Table I. (a) Very slight, (b) Slight. (c) Moderate. (d) Severe. (e) Rare. (f) Very rare.

the target spectra. The following equations present these parameters in detail.

$$S_a = \frac{Z.U.C.S}{R}.g \qquad (1)$$

$Z =$ According to Table I
$U = 1$ (Common building)
$S =$ According to Table II
$R = 1$ (Elastic spectrum)
$C =$ According to standard E.030

Fig. 10 illustrates the scaling of the Lima 17/Oct/1966 record from the Parque de la Reserva station for the Very Slight, Slight, Moderate, Severe, Rare, and Very Rare seismic demand levels. All seismic records listed in Table II were scaled using the same procedure, and the resulting peak ground accelerations (PGAs) for each demand level are summarized in Table III.

TABLE III
Peak Ground Accelerations (PGA) of the seismic records employed in seismic simulations.

Record	Station	Soil Profile Type	Seismic Demand					
			Very Slight	Slight	Moderate	Severe	Rare	Very Rare
			PGA (cm/s²)					
Lima_17/Oct/1966	Parque de la Reserva	S1	153	201	335	455	589	803
Huaraz_31/May/1970	Parque de la Reserva	S1	157	210	357	472	608	818
Lima_03/Oct/1974	Parque de la Reserva	S1	162	213	352	478	619	828
Arequipa_23/Jun/2001	César Vizcarra	S2	165	223	362	501	651	868
Pisco_15/Ago/2007	UNICA	S2	165	220	364	496	643	863
Lagunas_26/May/2019	SCIQU	S2	165	214	354	486	634	856
Sintético, SATREPS	-	S1	152	200	321	455	588	776

Note: Source REDACIS - CISMID.

2.2. CHARACTERISTICS OF EXPOSED DWELLINGS AND PROPOSED REINFORCEMENT

Fig. 11 presents typical floor plans of the masonry dwellings studied, illustrating that the shortest direction generally exhibits the lowest wall density and therefore governs the seismic response. This study examines fourteen masonry dwelling typologies, as detailed in Table IV [5], [9]. Each typology is analyzed for five wall-density values—1.6%, 2.3%, 2.8%, 3.4%, and 4.0%—resulting in a total of 70 dwellings in unretrofitted condition. The densities of 1.6%, 2.3%, and 2.8% correspond to the values obtained directly from the typical unretrofitted layouts. To explore configurations with greater lateral resistance and to increase the amount of wall area available for the strengthening intervention, two additional densities—3.4% and 4.0%—were generated by reducing the extent of wall openings while preserving the original wall distribution. This controlled range of densities enables a systematic evaluation of how variations in wall configuration influence the seismic capacity of the dwellings prior to retrofitting.

Similarly, each typology is evaluated in its retrofitted condition by applying a strengthening scheme consisting of a steel mesh and a cement–sand mortar coating on both sides of the wall. This retrofitting configuration is applied uniformly across all dwelling typologies to ensure comparability with the unretrofitted cases. Fig. 12 illustrates the retrofitting process applied to a masonry wall constructed with handmade solid bricks, as documented in the experimental program conducted by CISMID. In total, this results in 70 dwellings analyzed in the retrofitted condition.

The seismic capacity of the masonry dwellings, in both unreinforced and retrofitted conditions, was evaluated by calculating the average shear stress and the representative drift associated with the cracking, yielding, maximum, and ultimate damage states. Equation (2) and Table V present the formulation and parameters used to estimate the average shear stress for the unreinforced condition [13], whereas Equation (3) and Table VI provide the corresponding expressions for the retrofitted condition [14]. The representative drift limits adopted for each damage state were obtained from Table VII [14].

TABLE IV
Dwelling typologies unretrofitted and retrofitted.

N°	Unretrofitted	Retrofitted
1	001ML1	001ML1R (2)
2	001ML2	001ML2R (2)
3	002M2L1	002M2L1R (2.2)
4	002ML1.L2	002ML1.L2R (2.2)
5	002M2L2	002M2L2R (2.2)
6	003M2L1.L2	003M2L1.L2R (2.2.2)
7	003ML1.2L2	003ML1.2L2R (2.2.2)
8	003M3L2	003M3L2R (2.2.2)
9	004M2L1.2L2	004M2L1.2L2R(2.2.2.2)
10	004ML1.3L2	004ML1.3L2R (2.2.2.2)
11	004M4L2	004M4L2R (2.2.2.2)
12	005M2L1.3L2	005M2L1.3L2R(2.2.2.2.2)
13	005ML1.4L2	005ML1.4L2R (2.2.2.2.2)
14	005M5L2	005M5L2R (2.2.2.2.2)

Note: The specimen nomenclature indicates the structural configuration of each dwelling. The first three digits represent the number of stories. The labels *L1* and *L2* denote stories constructed with handmade solid bricks and industrial hollow bricks, respectively. The suffix *R* indicates retrofitted dwellings strengthened on both wall faces using steel mesh and cement–sand mortar. The numbers in parentheses specify the number of reinforced wall layers along the building height [5], [9].

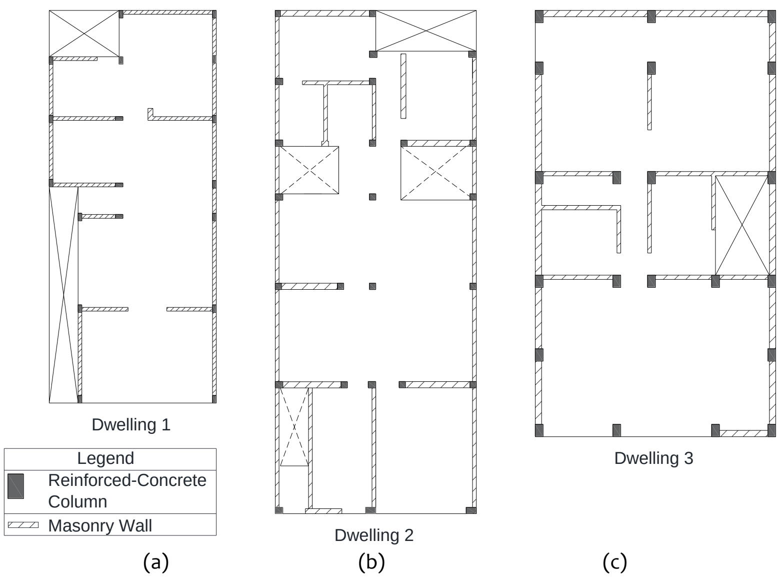

Fig. 11. Typical floor plans of the confined masonry dwelling typologies analyzed. (a) Dwelling 1. (b) Dwelling 2. (c) Dwelling 3.

(a) (b) (c) (d)

Fig. 12. Retrofitting process on both sides of the masonry wall using steel mesh and cement-sand mortar. (a) Steel mesh fabric. (b) Anchor drilling. (c) Steel mesh anchoring. (d) Mortar coating.

$$\frac{\tau}{f\prime m} = \beta_0 + \beta_1 (\frac{P_t.\sigma_y}{f\prime m})^{0.7} + \beta_2 \frac{P_{we}.\sigma_{wy}}{f\prime m} + \beta_3 \frac{\sigma_0}{f\prime m} .... (2)$$

$$F = \tau.L.t + \tau_R.n_R.t_R.L .... (3)$$

TABLE V
Constant coefficients of damages states

Coefficient	Cracking	Yielding	Maximum	Ultimate
β0	0.000	0.000	0.000	0.000
β1	0.000	0.000	0.054	0.221
β2	0.249	0.426	0.432	0.077
β3	0.221	0.175	0.290	0.503

Note: Source [13].

TABLE VI
Average shear stress values for reinforcement with steel mesh and cement-sand mortar of damage states

Damage State	t_R (MPa)	
	Cracking	Yielding
Cracking	0	0
Yielding	1.3	0.7
Maximum	1.6	1.15
Ultimate	2.1	1.75

Note: Source [14].

TABLE VII
Representative Drift (x10⁻³)

Unit brick	Cracking	Yielding	Maximum	Ultimate
Handmade solid	0.4	1.1	3.5	6.7
Industrial Tubular	0.4	0.8	1.5	2.3
Handmade solid retrofitted on both side	0.7	2.0	5.1	7.5
Industrial tubular retrofitted on both side	0.5	1.3	3.9	6.3

Note: Source [14].

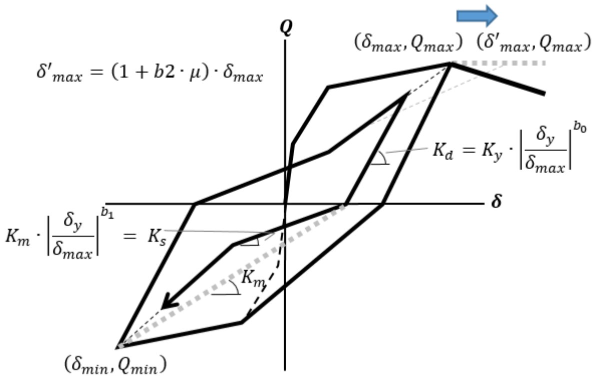

Fig. 13. Tetralinear hysteretic model [15].

Note: The tetralinear hysteretic model is governed by three hysteretic parameters: b_0, which controls stiffness degradation; b_1, which represents stiffness degradation associated with pinching effects; and b_2, which accounts for stiffness increase due to hardening effects related to crack closure during cyclic loading.

TABLE VIII
Representative Drift (x10⁻³)

Unit brick	b0	b1	b2
Handmade solid	0.55	0.04	0.01
Industrial Tubular	0.05	0.03	0.01
Handmade solid retrofitted on both side	0.36	0.39	0.01
Industrial tubular retrofitted on both side	0.25	0.36	0.01

Note: Source [14].

Fig. 14 presents the capacity curves for the dwelling typologies with a wall density of 1.5%. A pronounced reduction in lateral deformation capacity is observed at the story where the brick unit transitions along the height, reflecting the inherent structural irregularity of these configurations. This weakness is substantially mitigated after retrofitting, which produces a marked increase in both lateral strength and deformation capacity across all stories. Capacity curves were generated for all seventy unreinforced dwellings and their corresponding seventy retrofitted counterparts.

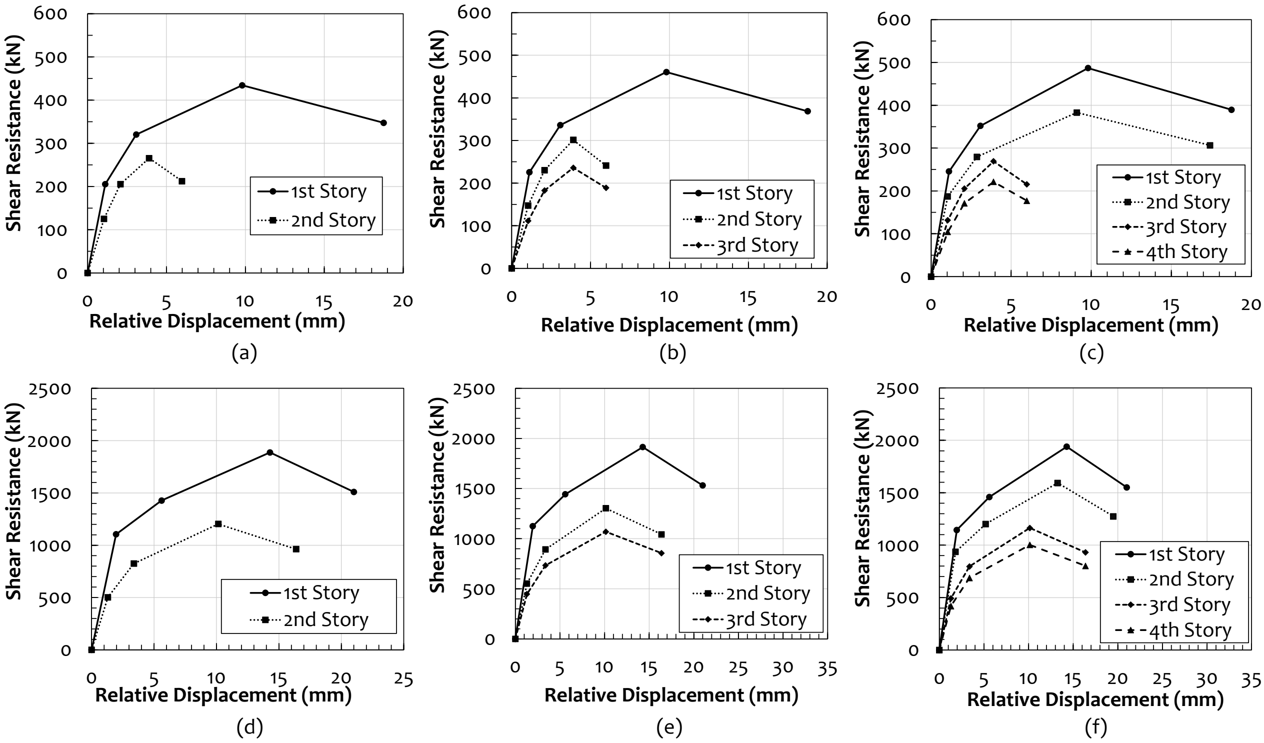

Fig. 14. Capacity curves of typologies with a wall density of 1.6%. (a) 002ML1.L2 (unretrofitted), (b) 003ML1.2L2 (unretrofitted). (c) 004ML1.3L2 (unretrofitted). (d) 002ML1.L2R (2.2) (retrofitted). (e) 003ML1.2L2R (2.2.2) (retrofitted). (f) 004ML1.3L2R (2.2.2.2) (retrofitted).

2.3. SEISMIC PERFORMANCE OF THE REPRESENTATIVE SAMPLE OF EXPOSED DWELLINGS

A total of 5,880 nonlinear time-history (TH) simulations were performed, corresponding to 70 unreinforced dwellings and 70 retrofitted dwellings. Each dwelling was subjected to 24 seismic records for S1 soil and 18 for S2 soil. The structural response was computed using a unidirectional lumped-mass model with a single degree of freedom (SDOF), which is appropriate for low-rise confined masonry dwellings whose behavior is governed primarily by shear deformations.

The nonlinear behavior of the unretrofitted and retrofitted masonry walls was represented using a tetralinear hysteretic model with strength and stiffness degradation, calibrated from the capacity curves previously obtained for each dwelling typology. These capacity curves explicitly incorporate the influence of brick type and the corresponding drift capacities. The hysteretic parameters were taken directly from experimental studies conducted by CISMID as show in Table VIII, ensuring that the TH simulations reproduce the cyclic response observed in laboratory testing and numerical calibration reported in related research [13].

No reinforced-concrete hysteretic elements were included because the lateral resistance of the dwellings is governed primarily by the confined masonry walls. The contribution of the boundary confinement columns is already embedded in the shear-strength formulations used for both unretrofitted and retrofitted conditions. Isolated reinforced-concrete columns—present only in a limited number of typologies—do not significantly affect the global lateral response and were therefore excluded from the analytical model. Calibration was verified by ensuring that the pushover-derived capacity curves of the SDOF model match the backbone curves of each typology within the relevant drift ranges.

The interstory drifts obtained from the TH analyses were normalized according to the brick type assigned to each story, producing drift-based indices ranging from 0 to 5. Thresholds of 1, 2, 3, and 4 correspond to Slight, Moderate, Extensive, and Collapse damage states, respectively [16]. Fig. 15 summarizes the simulation results for the unreinforced and retrofitted dwelling typologies for both S1 and S2 soil conditions. For S1 soil, the percentage of collapsed dwellings decreases from 81.43% to 10.00% under a Severe demand, and from 95.71% to 47.14% under a Very Rare demand. For S2 soil, collapse reductions follow a similar trend, decreasing from 88.57% to 14.29% under Severe demand and from 94.29% to 55.71% under Very Rare demand.

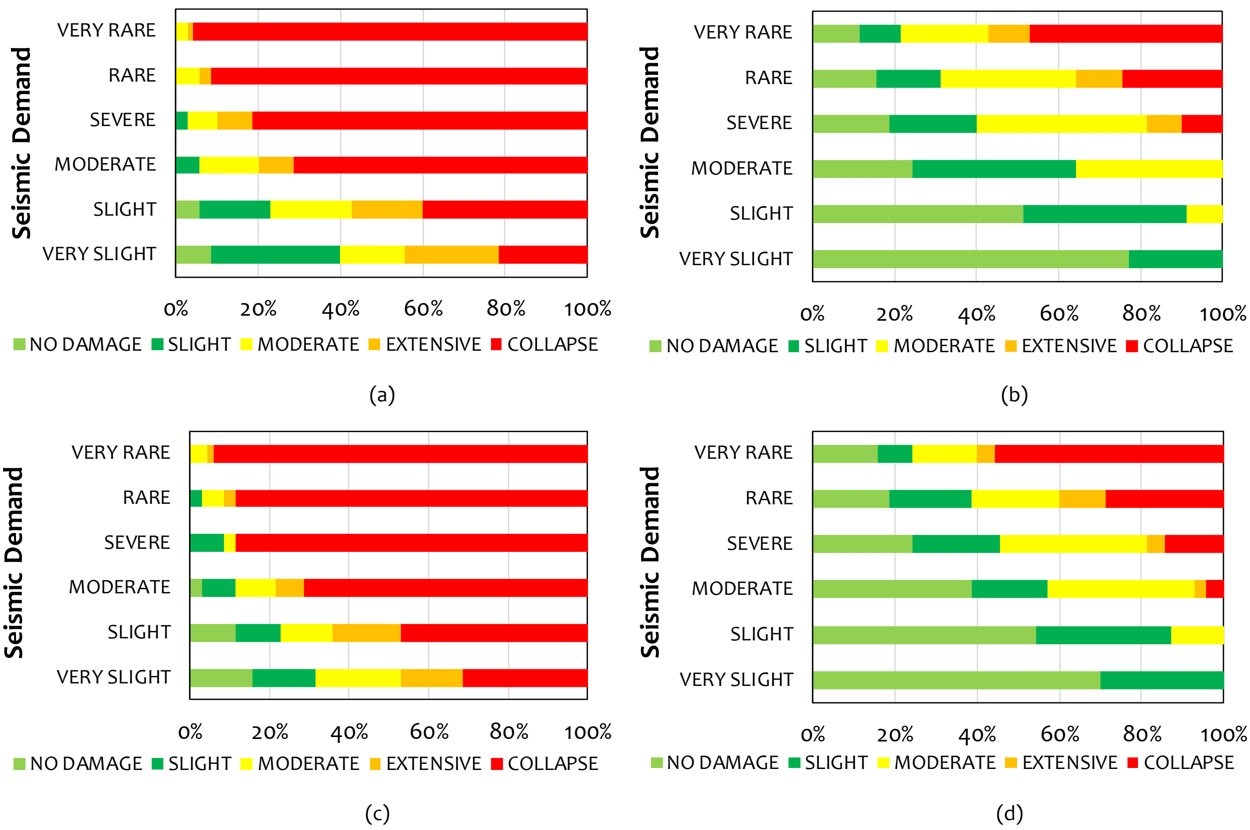

Fig. 15. Summary of damage levels from simulations for typologies with wall densities of 1.6%, 2.3%, 2.8%, 3.4%, and 4.0%. (a) Unretrofitted dwellings on S1, (b) Retrofitted dwellings on S1. (c) Retrofitted dwellings on S2. (d) Retrofitted dwellings on S2.

CONCLUSIONS

- The seismic capacity of confined masonry dwelling typologies is significantly improved in terms of lateral strength and deformation capacity when retrofitted with steel mesh and cement–sand mortar. This improvement is particularly pronounced in dwellings exhibiting changes in brick type along the height, which are highly vulnerable in the unretrofitted condition.
- A greater number of damaged dwellings was observed in the simulations conducted on intermediate soil (S2), due to its broader range of spectral amplification periods compared to rigid soil (S1). This effect was consistently observed across the analyzed seismic demand levels.
- Most of the analyzed dwelling typologies exhibit a substantial reduction in damage levels when retrofitted with steel mesh and cement–sand mortar, especially under Severe, Rare, and Very Rare seismic events. However, some dwellings with an insufficient number of walls remain unable to adequately withstand these high seismic demands, even after retrofitting.
- A key contribution of this study is the systematic extension of wall-density cases evaluated for both unretrofitted and retrofitted dwellings. The results show that very low wall densities remain vulnerable under severe and very rare seismic demands, even after strengthening, whereas increased wall density leads to a clear reduction in damage and collapse probabilities. Although no regulatory changes are proposed, these findings highlight wall density as a critical parameter governing seismic performance.
- Compared to previous studies, this work builds upon established dwelling configurations by extending the range of wall-density scenarios analyzed and by presenting the methodology in greater detail. The comparative evaluation of unretrofitted and retrofitted dwellings across multiple density levels provides additional quantitative insight into the influence of wall configuration on seismic damage and collapse outcomes.

ACKNOWLEDGMENTS

The author gratefully acknowledges Dr. Miguel Díaz for his valuable technical guidance and critical contributions throughout this research. Appreciation is also extended to Erika Flores, Michel Amancio, and

Steven Roman for their support and technical insights. This research was funded by FONDECYT, whose support is sincerely acknowledged. The author also thanks the principal investigators, research assistants, and technical staff of CISMID for their collaboration and assistance during the development of this study.

REFERENCES

[1] M. Díaz, "Análisis estadístico y área de estudio seleccionada representativa de Lima y Callao" [Statistical Analysis and Selected Study Area Representative of Lima and Callao], Centro Peruano-Japonés de Investigaciones Sísmicas y Mitigación de Desastres (CISMID), Universidad Nacional de Ingeniería, Lima, Perú, Tech. Rep., May 2019.

[2] M. Diaz, C. Zavala, J. Gallardo and L. Lavado, "Experimental Study of Non-Engineered Confined Masonry Walls Retrofitted with Wire Mesh and Cement-Sand Mortar", The 16th World Conference on Earthquake Engineering, Santiago de Chile, 2017.

[3] C. Zavala, C. Honma, P. Gibu and J. Gallardo, "Full Scale on Line Test on Two Story Masonry Building using Handmade Bricks" The 13th World Conference on Earthquake Engineering, Vancouver, 2004.

[4] R. Salinas and F. Lazares, "Seismic Performance of Confined Masonry Buildings with Tubular Bricks in Developing Areas" The 14th World Conference on Earthquake Engineering, Beijing, 2008.

[5] M. Diaz and E. Flores, "Structural Assessment of Confined Masonry Retrofitting Under Multi-Seismic Scenarios in Metropolitan Lima Area", The 17th World Conference on Earthquake Engineering, Sendai, 2020.

[6] C. Zavala, M. Diaz, E. Flores and L. Cardenas, "Damage limit states for confined masonry walls based on experimental test" TECNIA, vol. 29(2), pp. 135–141, Jul-Dec. 2019.

[7] C. Zavala, P. Gibu, M. Diaz and D. Gruber, "Feasibility of electrowelded wire mesh and mortar in the Retrofitting of Damaged Dwellings because of Extreme Lateral Cyclic Loading" Proceedings of XVII National Congress of Civil Engineering, Peru, 2009.

[8] SENCICO, "Technical Standard E.030 Seismic-Resistant Design". Ministry of Construction, Housing and Sanitation. Peru. 2018.

[9] E. Flores, M. Diaz and C. Zavala, "Probabilistic Seismic Risk Assessment using Fragility Function for Dwelling in Metropolitan Lima Area" The 17th World Conference on Earthquake Engineering, Sendai, 2020.

[10] ASCE 41-23, "Seismic Evaluation and Retrofit of Existing Buildings (ASCE standard ASCE/SEI 41-23)". American Society of Civil Engineers. 2023.

[11] M. Díaz, "Set de curvas de peligro sísmico en Lima con las fuentes sísmicas de influencia" [Set of seismic hazard curves in Lima considering influencing seismic sources], Centro Peruano-Japonés de Investigaciones Sísmicas y Mitigación de Desastres (CISMID), Universidad Nacional de Ingeniería, Lima, Perú, Tech. Rep., May 2019.

[12] Centro Peruano–Japonés de Investigaciones Sísmicas y Mitigación de Desastres (CISMID), "REDACIS: Red de Acelerógrafos de CISMID," [Online]. Available: https://www.cismid.uni.edu.pe/ceois/redacis/red/.

[13] M. Diaz, C. Zavala and E. Flores and L. Cardenas, "Development of analytical models for confined masonry walls based on experimental results in Lima city" TECNIA, vol. 29(2), pp. 23–29, Jul-Dec. 2019.

[14] CISMID, "Analysis Report on the Improvement of Seismic Resistance Capacity in Confined Masonry Walls Retrofitted with Steel Mesh and Mortar" Japan-Peru Center for Earthquake Engineering Research and Disaster Mitigation. Program 0068 – Reduction of Vulnerability and Emergency Response to Disasters, Technical Report. 2020

[15] T. Saito, "Technical Manual of Structural Earthquake Response Analysis (STERA)." Toyohashi University of Technology, Tech. Rep. Version 6.1, May 2019. https://rc.ace.tut.ac.jp/saito/software-e.html

[16] L. Lopez, "Effectiveness Analysis of the Reinforcement of Confined Masonry Dwellings Using Steel Mesh and Mortar in Metropolitan Lima" *National University of Engineering*, Lima-Peru. 2023.